

1981

Quantum effects in spin dynamics of one dimensional systems

H. Beck

M. W. Puga

Gerhard Müller

University of Rhode Island, gmuller@uri.edu

Follow this and additional works at: https://digitalcommons.uri.edu/phys_facpubs

Terms of Use

All rights reserved under copyright.

Citation/Publisher Attribution

Beck, H., Puga M. W., & Müller, G. (1981). Quantum effects in spin dynamics of one-dimensional systems. *J. Appl Phys.*, 52, 1998-2003. doi: 10.1063/1.329595

Available at: <http://dx.doi.org/10.1063/1.329595>

This Article is brought to you for free and open access by the Physics at DigitalCommons@URI. It has been accepted for inclusion in Physics Faculty Publications by an authorized administrator of DigitalCommons@URI. For more information, please contact digitalcommons@etal.uri.edu.

Quantum effects in spin dynamics of one dimensional systems

H. Beck^a and M. W. Puga^a

Institute of Physics, University of Neuchâtel, CH-2000 Neuchâtel, Switzerland

G. Müller^a

Institute for Theoretical Physics, University of Basel, CH-4056 Basel, Switzerland

We present a review of recent results concerning dynamical spin correlation functions of quantum spin chains with nearest neighbor exchange interactions. Zero and finite temperature results, as well as the influence of a magnetic field are discussed for $s = 1/2$, with special emphasis on quantum effects which can be observed experimentally. We also investigate the dependence on spin quantum number between extreme quantum ($s = 1/2$) and classical ($s = \infty$) systems.

PACS numbers: 75.10.Jm, 75.30.Et, 76.60.Es

1. INTRODUCTION

Our intuitive picture of spin dynamics is usually based on a ground state arrangement of some classical unit vectors and oscillations around this configuration. Spin wave theory is indeed successful for describing the low T properties of 3-d ordered magnets. Spin dynamical theories in 1-d have for a long time relied on the same classical approach [1]. For a classical system the T = 0 dynamics is usually governed by sharp spin wave excitations [2] as for d = 3. At finite T computer simulations of the spin dynamics are available [3].

On the other hand there is now plenty of evidence - experimental and theoretical - that quantum effects are important at low T, causing qualitative differences between classical and quantum spin chains. Evidently these effects are most important for $s = 1/2$. Fortunately enough, this extreme quantum case is also the one which is amenable to various analytic and numerical approaches, which have shed considerable light on the low T dynamics in the past few years. This is a gratifying success, although rigorous solutions are still only available in rare special instances. Much less has been done in the wide domain $1/2 < s \leq \infty$.

We consider the Hamiltonian

$$H = J \sum_{\ell=1}^N \{ (1+\gamma) S_x(\ell) S_x(\ell+1) + (1-\gamma) S_y(\ell) S_y(\ell+1) + \Delta S_z(\ell) S_z(\ell+1) - h S_z(\ell) \} \quad (1)$$

of the so-called "XYZ-chain" of N spins at sites ℓ and periodic boundary conditions. Many quasi 1-d magnets can be described by (1) in the T-range where interchain coupling is weak [1]. CPC and the copper salts $\text{CuSO}_4 \cdot 5\text{H}_2\text{O}$ etc. are examples for $s = 1/2$, $\gamma = 0$, $\Delta = 1$ (isotropic Heisenberg antiferromagnet, HBAF), whereas CoCl_2 has $s = 3/2$, $\gamma = 0$, $\Delta = 10$.

The dynamical properties of such systems are best characterized by spin correlation functions of the type

$$G_r(q, \omega) \equiv \sum_{\ell} e^{-iq\ell} \int dt e^{i\omega t} \langle S_r(\ell, t) S_r(0, 0) \rangle. \quad (2)$$

They can be measured by two experimental techniques :

(i) Inelastic neutron scattering produces $G_r(q, \omega)$ or combinations for various spin components r [1]

(ii) The "spin-lattice relaxation time" T_1 of NMR signals is determined by the autocorrelation functions

$$\phi_r(\omega) \equiv \int dt e^{i\omega t} \langle S_r(0, t) S_r(0, 0) \rangle = \frac{1}{N} \sum_q G_r(q, \omega) \quad (3)$$

for $\omega \approx 0$.

The main methods to investigate 1-d spin dynamics are :

- (i) Semiclassical expansions in $1/s$, based on the Holstein-Primakoff transformation [4]
- (ii) Fermion representation of $s = 1/2$ spin chains [5] and application of techniques in the framework of Luttinger's approximation to interacting Fermion chains [6,7]
- (iii) Bethe ansatz techniques for evaluating eigenvalues of (1) for $\gamma = 0$ [8-11]
- (iv) Numerical diagonalization of (1) for finite chains ($N \leq 10$), yielding eigenvalues E_λ and eigenstates $|\lambda\rangle$, which allows us to represent G_r as

$$G_r(q, \omega) = \frac{2\pi}{Z} \sum_{\lambda\lambda'} e^{-\beta E_\lambda} |\langle \lambda | S_r(q) | \lambda' \rangle|^2 \delta(\omega + E_\lambda - E_{\lambda'}). \quad (4)$$

We now present various recent results concerning 1-d quantum spin dynamics. Except for the few cases, where exact results can be found, the strategy is to combine the above mentioned methods in order to obtain as complete as possible a description of the behavior of G_r and ϕ_r .

2. VARIOUS RESULTS

We mainly concentrate on "isotropic chains" ($\gamma = 0$), for which the Bethe ansatz technique is devised and the rotational invariance with respect to the z-axis simplifies the classification of the eigenstates. We discuss various domains of the parameters Δ , h , T separately.

(a) $h = 0, T = 0$ ($\gamma = 0$)

$s = 1/2, 0 \leq \Delta \leq 1$: In this range we find the isotropic XY-chain ($\Delta = 0$), for which G_z can be evaluated exactly, and the HBAF ($\Delta = 1$). For the latter we have previously presented the spin wave continuum (SWC) approximation to G_r and its implications for various static

quantities [12,13]. Here we generalize this approach to the full range $0 \leq \Delta \leq 1$. Finite chain work has shown that, at $T = 0$, the most important excited states $|\lambda'\rangle$ coupling to the ground state form continua (in the limit $N \rightarrow \infty$) of the form shown in Fig. 1 for G_Z and G_X , extending between boundaries $\epsilon_1(q)$ and $\epsilon_2(q)$. States above $\bar{\epsilon}_2$ contribute much less to the $T = 0$ dynamics. In the Bethe formalism ϵ_1 and $\bar{\epsilon}_2$ and the density of states can be calculated. However, the matrix elements in (4) are only known for small N . In order to find the frequency dependence of G_T between ϵ_1 and $\bar{\epsilon}_2$ we make use of the relation between 1-d quantum spin chains and the 2-d Baxter model [14], which allows the identification of critical Baxter exponents with exponents governing the frequency-wave vector behavior of 1-d spin correlation functions [6]. We postulate the following forms :

$$G_Z(q, \omega) = A(\Delta) \theta(\omega - \epsilon_1(q)) \theta(\epsilon_2(q) - \omega) \cdot (\omega^2 - \epsilon_1^2(q))^{-\alpha} (\epsilon_2^2(q) - \omega)^{\alpha - \frac{1}{2}} \quad (5)$$

$$G_X(q, \omega) = B(\Delta) \theta(\omega - \epsilon_1(q)) \theta(\epsilon_2(q) - \omega) \cdot (\omega^2 - \epsilon_1^2(q))^{-\beta} (\epsilon_2^2(q) - \omega)^{\beta - \frac{1}{2}} + C(\Delta) \theta(\omega - \epsilon_1(q)) \theta(\bar{\epsilon}_2(q) - \omega) (\omega^2 - \epsilon_1^2(q))^{-\nu} (\bar{\epsilon}_2^2(q) - \omega)^{\nu - \frac{1}{2}} \quad (6)$$

Here

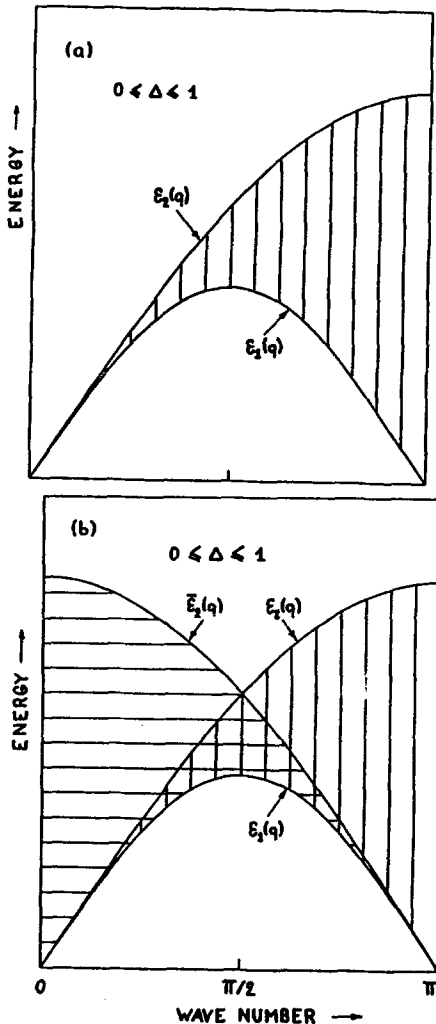


Fig. 1 Spin wave continua contributing to $G_Z(q, \omega)$ (a) and $G_X(q, \omega)$ (b) at $T = 0$. The boundaries ϵ_1 , ϵ_2 , $\bar{\epsilon}_2$ are those of equ's. (5) and (6).

$$\epsilon_1(q) = \frac{\pi J \sin \theta}{2\theta} \sin q, \quad \epsilon_2(q) = \frac{\pi J \sin \theta}{\theta} \sin \frac{q}{2},$$

$$\bar{\epsilon}_2(q) = \frac{\pi J \sin \theta}{\theta} \cos \frac{q}{2}, \quad \cos \theta = \Delta.$$

The form of the exponents

$$\alpha = (\pi/2 - \theta)/(\pi - \theta), \quad \beta = 1/2 + \theta/2\pi, \quad \nu = \theta^2/(2\pi\theta - 2\pi^2) \quad (7)$$

is suggested by ref. 6. Special values are

$$\Delta = 0 : \quad \alpha = 0, \quad \beta = 3/4, \quad \nu = -1/4$$

$$\Delta = 1 : \quad \alpha = 1/2, \quad \beta = 1/2, \quad \nu = 0.$$

The unknown constants A, B, C can be determined by the sum rule relating the first moment of G_T to static correlation functions [15], which can be evaluated by the Hellman-Feynman theorem since the Δ -dependence of the ground state energy is known.

The consequences of (5) and (6) are best seen in Fig. 2 and 3, presenting the line shapes for G_Z and G_X , respectively. In the limit $\Delta = 1$ ($G_X = G_Z$) we recover our previous result : there is a peak at the lower boundary (the des Cloizeaux-Pearson frequencies [10]) and for $q \leq \pi$ the spectrum has a considerable tail towards the higher boundary. This is an intrinsic quantum effect due to the presence of a whole continuum of spin waves. At $\Delta = 0$, G_Z agrees with exact results [16,17]. For intermediate Δ , G_Z has two peaks, one at each boundary. This remarkable feature should be best visible in the neutron spectra of a material with $\Delta \approx 0.5$. In G_X the first part of (6), diverging at the lower boundary, is dominant for $q \leq \pi$. However, for small q both SWC contribute, yielding again two peaks, which should be best observable for small Δ (due to the Δ -dependence of B and C).

The corresponding static correlation functions $I_T(q)$ give the integrated neutron intensities. I_Z vanishes for $q \rightarrow 0$ and is finite for all q for $\Delta < 1$, whereas at $\Delta = 1$ there is a logarithmic divergence for $q \rightarrow \pi$. As previously discussed [13] this differs from the classical $(\pi - q)^{-1}$ behavior and fits experiments quite well. I_X goes like $(\pi - q)^{1-2\beta}$ for $\Delta < 1$. At $\Delta = 0$ the corresponding large R decay of S_X -correlations turns out to be [18]

$$I_X(R) = 0.1470 (-1)^R / R^{1/2} + \dots, \quad (8)$$

in remarkable agreement with the exact result [19]

$$I_X(R) = 0.1471 (-1)^R / R^{1/2} + \dots \quad (9)$$

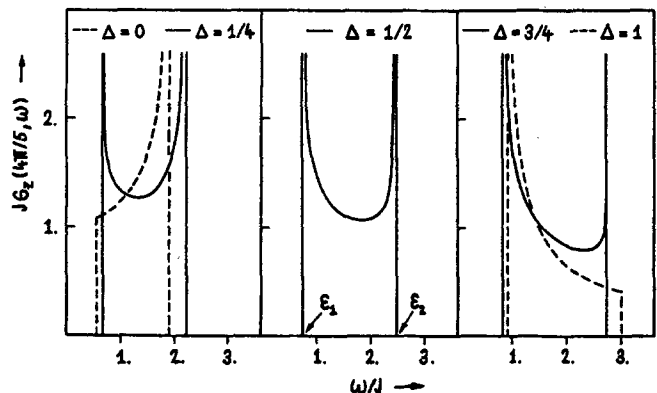


Fig. 2 Line shape of $G_Z(q, \omega)$ for $q = \frac{4\pi}{5}$ and varying Δ .

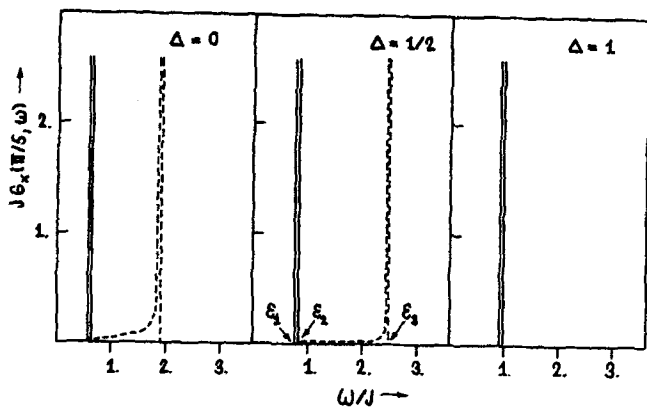


Fig. 3 Line shape of $G_x(q, \omega)$ for $q = \frac{\pi}{5}$ and varying Δ .

The static susceptibility $\chi_r(q)$ is the ω^{-1} moment of G_r . χ_z diverges logarithmically at $q = \pi$ for $\Delta = 0$, whereas

$$\chi_z(q) \propto (\pi - q)^{-2\alpha} \quad \text{for } \Delta > 0. \quad (10)$$

The exact form of $\chi_z(0)$ is [20]

$$\chi_z^{-1}(0) = J\pi(\pi - \theta)\sin\theta/\theta. \quad (11)$$

Our result deviates by a few percent only (except near $\Delta = 1$, where the deviation grows to about 15%). The small discrepancy is due to the neglect of states above the SWC. Near the zone boundary we find $\chi_x \propto (\pi - q)^{-2\beta}$.

Last, but not least, the autocorrelation functions $\phi_r(\omega)$ can be evaluated. For small ω :

$$\phi_z \propto \omega^{1-2\alpha} \quad (\alpha < \frac{1}{2}) \quad \Delta < 1 \quad (12a)$$

$$\phi_x \propto \omega^{1-2\beta} \quad (\beta > \frac{1}{2}) \quad \Delta < 1 \quad (12b)$$

$$\phi_x = \phi_z = \frac{A}{\pi} + O(\omega) \quad \Delta = 1 \quad (13)$$

There is thus a qualitative difference between the finite limit for $\Delta = 1$ and the behavior for all other Δ , which should have its bearings on NMR experiments at low fields.

It seems worthwhile to compare these results, which - though not quite rigorous - seem to exhibit the basic features of quantum spin dynamics, to classical spin wave theory. There the dispersion relation for oscillations around the Néel ground state is

$$\omega_r(q) = 2sJ\sqrt{(1 \mp \cos q)(1 \pm \Delta \cos q)} \quad (14)$$

where the upper (lower) sign is for $r = z$ ($r = x$), the spins being assumed to lie parallel to the y -direction at $T = 0$. The correlation functions

$$G_r(q, \omega) = I_r(q) 2\pi \delta(\omega - \omega_r(q)) \quad (15)$$

are in sharp contrast to the asymmetric line shapes for $s = \frac{1}{2}$, at least for large q . Moreover $\omega_r(q)$ has a gap at $q = 0$ ($r = x$) or $q = \pi$ ($r = z$) for $0 < \Delta < 1$, whereas for $s = \frac{1}{2}$ there is spectral weight down to $\omega = 0$ in both cases. It is interesting to note, however, that for $s = \frac{1}{2}$ the main spectral weight of $G_z(\pi, \omega)$ and $G_x(0, \omega)$ is also at non-zero frequencies for $\Delta < 1$, which leads to an "apparent gap". I_r and χ_r also behave differently. For example, the classical $\chi_z(\pi)$ is finite for $\Delta < 1$ in contrast to (10) for $s = \frac{1}{2}$.

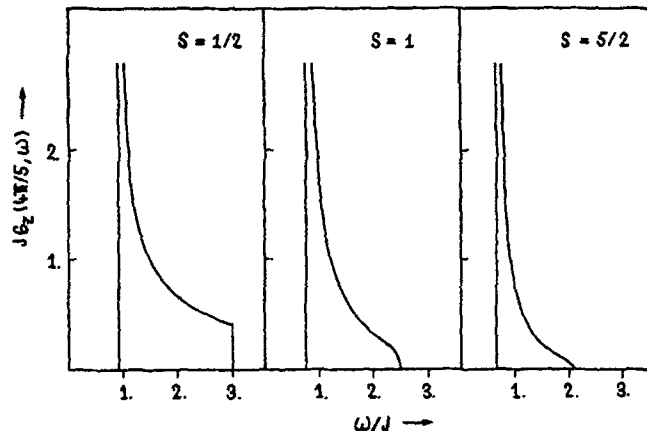


Fig. 4 Line shape of $G_z(q, \omega)$ for $q = \frac{4\pi}{5}$ and various s .

Obviously it would be extremely interesting to know the "interpolating" behavior for $s > \frac{1}{2}$. There are prominent examples for higher spin quantum numbers (CsNiF₃ has $s = 1$, TMMC $s = \frac{5}{2}$). The success of the SWC approximation has prompted us to try the following generalization:

$s > \frac{1}{2}$, $\Delta = 1$: Finite chain work for $s = 1$ shows that the main spectral weight for G_r is still concentrated between two boundaries of the same shape ($\sin q$ and $\sin q/2$). Moreover, Mikeska's $1/s$ expansion [4] yields a low ω behavior consistent with (5) with $\alpha = \alpha(s) = 1 - (\pi s)^{-1} + \dots$. We thus propose the form (5) for G_r to be valid for all s ; $\epsilon_1, \epsilon_2, A$ and α now depending on s . This ansatz is in fact compatible with the first moment sum rule, and letting $\alpha(s)$ vary between $\frac{1}{2}$ ($s = \frac{1}{2}$) and 1 ($s \rightarrow \infty$) we can interpolate between the SWC form established for $s = \frac{1}{2}$ and the classical limit (15) for $s \rightarrow \infty$. We correctly find the classical forms of I_r and χ_r in the same limit. Fig. 4 shows the line shapes for $s = \frac{1}{2}, 1, \frac{5}{2}$. The asymmetry gradually diminishes due to the changing exponent α . Early neutron data on TMMC [21] seem indeed to show a small asymmetry near $q = \pi$. Evidently a systematic study of the s -dependence of experimental data is highly desirable.

The low frequency behavior of $\phi_r(\omega)$ also shows an interesting variation with s . Our SWC ansatz yields

$$\phi_r(\omega) \propto \omega^{1-2\alpha} \quad (\text{for small } \omega) \quad (16)$$

Thus, for $s = \frac{1}{2}$, $\phi_r(0)$ is finite, whereas for $s > \frac{1}{2}$ it diverges. This, for the first time, sheds some light on the very different behavior of the NMR relaxation time T_1 for TMMC [22] and the copper salts [23]. T_1^{-1} is determined by the values $\phi_r(\omega \approx 0)$. Thus for $s = \frac{5}{2}$, T_1^{-1} should diverge for $T \rightarrow 0$, whereas for $s = \frac{1}{2}$ it should tend to a finite limit, as the experiments indeed show.

Finally it is interesting to speculate that the forms (5), (6) are good approximations to G_r in the full range $0 \leq \Delta \leq 1$ and $\frac{1}{2} \leq s < \infty$, the various parameters like $\epsilon_i(q)$ etc., then depending on both, Δ and s . However, we need more information about the static quantities in this domain of Δ and s , in order to determine these parameters by the help of the moments of G_r .

$s = \frac{1}{2}$, $\Delta > 1$: For this domain (HB-Ising AF) Johnson et al. [14] have given explicit formulae for the continuum boundaries. There is now a gap above the ground state. The existence of a continuum suggests similar forms as (5), (6) for G_r . However, in this case, (5) and (6) are incompatible with sum rules, so a different ansatz has to be found. Ishimura and Shiba [24] performed a

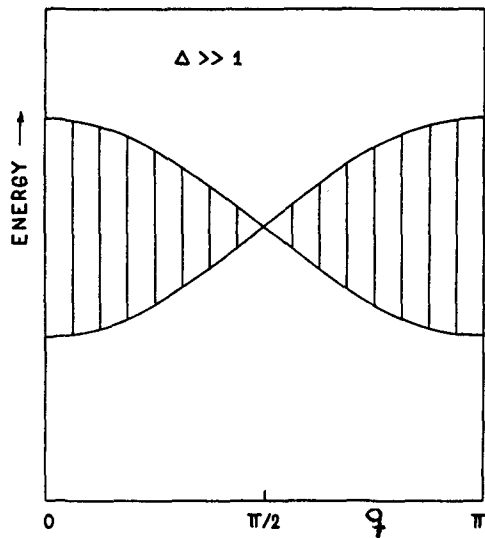


Fig. 5 Continuum of excited states for $\Delta \gg 1$. More details are found in ref. 24.

perturbation calculation starting from the solvable Ising limit $\Delta = \infty$. Fig. 5 shows their continuum of states (in agreement with [14]), corresponding, in this case, to moving domain walls between adjacent anti-ferromagnetic domains. The line shapes are symmetric for G_z and somewhat asymmetric for G_x . Recent neutron experiments on CsCoCl_3 [25] clearly demonstrate the contribution of a continuum to G_x , but they suggest that the asymmetry is in fact larger than predicted [24]. In fact a spectral distribution of the type (5) with possible discontinuities or divergences at the boundaries may be closer to the reality when Δ is not too close to the Ising limit.

$s = \frac{1}{2}, -1 \leq \Delta < 0$: In this domain a SWC and a sequence of bound state branches are predicted [14]. The first branch appears at arbitrary small $|\Delta|$, but the following ones successively show up at given values of Δ . Finite chain calculations indicate, however, that only the first bound state branch contributes significantly to the $T = 0$ dynamics in addition to the SWC, see Fig. 6. Near the ferromagnetic limit $\Delta = -1$, the dominant contribution to G_z then comes from this single branch of bound states. Thus it seems reasonable to combine (5) with a separate discrete contribution of the form (15) from the bound states. The exponent for the SWC can again be found from the Baxter model and Luttinger model calculations [6,26], but the bound state matrix elements would have to be evaluated for large N in a different way (e.g. perturbation theory around $\Delta = 0$). In the limit $\Delta = -1$ (isotropic ferromagnet, FM) the SWC vanishes, the first bound state branch goes into the FM spin wave branch and G_x has the classical form (15). In this limit the other bound states do not contribute to the $T = 0$ dynamics. In a similar way G_T may develop in this Δ -domain for higher s : the SWC will gradually lose importance, leading to the limit (15) with the upper sign of (14).

(b) $h \neq 0, T = 0$

For $|\Delta| \leq 1$, the surprising fact is that the lowest excitations in finite field [27,28] follow a dispersion curve $\epsilon_1(q)$, qualitatively different from the classical case: there is a wave vector $q^* = \pi(1 - \sigma(h))$ at which $\epsilon_1 = 0$ ($\sigma = \text{magnetization}$). This is perhaps the most mysterious quantum effect: a totally homogeneous external field imposes upon the system a special wave vector $q^*(h)$ which continuously runs through the Brillouin zone with varying h . One

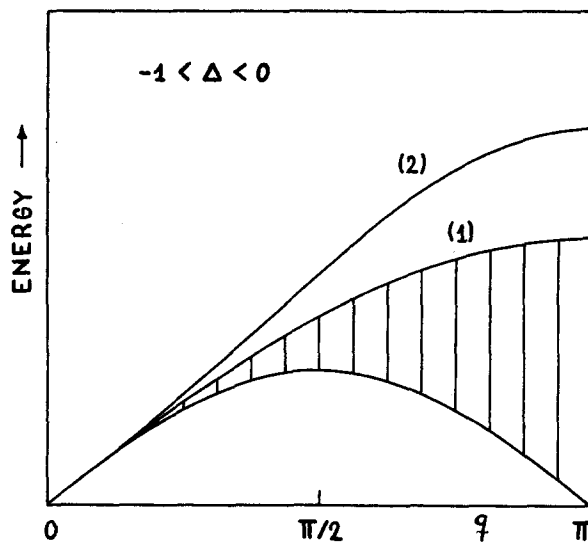


Fig. 6 Spin wave continuum (1) and branch of bound states (2) dominating $G_z(q, \omega)$ for $\Delta \leq 0$.

is therefore prepared to encounter quite complicated patterns in G_x . Exact results for $\Delta = 0$ [16,17] indeed reveal the existence of two continua contributing to G_z :

$$G_z(q, \omega) = \frac{\theta(\epsilon_2(q) - \omega)\theta(\omega - \epsilon_1(q))}{(4J^2 \sin^2(q/2) - \omega^2)^{1/2}} \quad 0 \leq q \leq \pi\sigma \quad (17)$$

$$= \frac{\theta(\epsilon_3(q) - \omega)[\theta(\omega - \epsilon_1(q)) + \theta(\omega - \epsilon_2(q))]}{(4J^2 \sin^2(q/2) - \omega^2)^{1/2}} \quad \pi\sigma \leq q \leq \pi$$

with

$$\epsilon_1(q) = 2J \left| \sin \frac{q}{2} \cos \left(\frac{q}{2} + \pi\sigma \right) \right|$$

$$\epsilon_2(q) = 2J \sin \frac{q}{2} \cos \left(\frac{q}{2} - \pi\sigma \right)$$

$$\epsilon_3(q) = 2J \sin \frac{q}{2}, \quad h = \sin(\pi\sigma)$$

For $q < 2\pi\sigma$ one SWC contributes with a divergence at the upper boundary. For $q > 2\pi\sigma$ both SWC contribute. There is a discontinuity at the "interface" and a divergence at the upper limit.

For $\Delta = 1$ we have to rely on finite chains, exploiting the selection rules concerning the quantum numbers S and S_z of total spin and its z -component [29]. With increasing h the ground state gradually moves from $S = S_z = 0$ through a sequence of states $|S, S_z = S\rangle$ with $S = 1, 2, \dots$, until at the critical field $h_c = 2$ it is the FM state $|\frac{N}{2}, \frac{N}{2}\rangle$. Given such a ground state $|S, S\rangle$ the following excited states can occur in (4):

$$G_z: \quad |S+1, S\rangle \quad \text{and} \quad |S, S\rangle, \quad \text{since } \Delta S_z = 0, \Delta S = 0, 1,$$

$$G_x: \quad |S+1, S+1\rangle, \quad |S+1, S-1\rangle, \quad |S, S-1\rangle, \quad |S-1, S-1\rangle,$$

$$\text{since } \Delta S_z = \pm 1.$$

It is again possible to identify in Bethe's formalism those subclasses of these six sets of states which are of spin wave character (states of "class C" [8]) and to calculate the boundaries of these SWC [29]. However, while for $h = 0$ class C states gave by far the dominant contribution to G_T , this is gradually less so with increasing field. Therefore a SWC approximation for G_T may be less reliable for $h \neq 0$.

At this stage a novel point of view arises concerning the extrapolation of finite chain results to large N . Although all the above listed excited states are allowed by selection rules, the Wigner-Eckart theorem, providing relations between matrix elements, shows that some of them are smaller by $(N\sigma)^{-1}$ or $(N\sigma)^{-2}$ than others. The "big" matrix elements cannot increase without bound for $N \rightarrow \infty$, due to sum rules, therefore the "small" ones will vanish in the thermodynamic limit. This yields "macroscopic" selection rules, which are more restrictive than those for S and S_z used above and simplify the situation for $N \rightarrow \infty$. In Fig. 7 we present the surviving SWC for G_z and G_x . Unfortunately we do not have enough information from calculations in the Fermion picture, such as ref. 6 for $h = 0$, in order to write down concrete expressions like (5), (6) for $h \neq 0$, but the following remarks can be made:

G_z : Matrix elements for finite chains suggest a divergence at the lower boundary of the SWC which remains for $N \rightarrow \infty$ and a discontinuity at ϵ_2 , the upper boundary. But we have to bear in mind that even for moderate fields, states above ϵ_2 - not of SW type - will also appreciably contribute. Note the interesting fact that the (dashed) upper boundary of the SWC at $h = 0$ disappears abruptly at $h = 0^+$ in the limit $N \rightarrow \infty$. This vividly demonstrates the critical properties of the point $h = 0, T = 0$ in the phase diagram. It also suggests experiments on systems whose magnetic chains

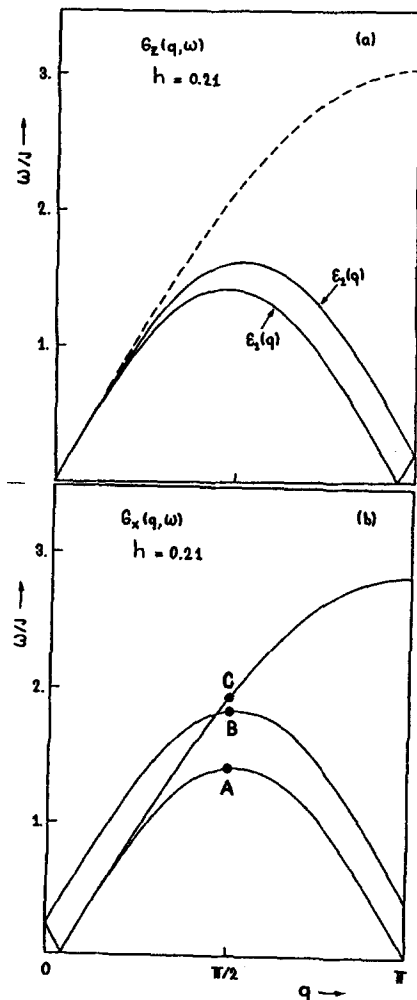


Fig. 7 Spin wave continua in a finite field in the thermodynamic limit, contributing to G_z (a) and G_x (b). For A, B, C see text. The dashed line in (a) indicates the $h = 0$ upper SWC boundary which becomes meaningless at finite h .

are interrupted by impurities. The finite N segments of such chains may then reveal the existence of those continua that are suppressed for $N \rightarrow \infty$.

G_x : Two SWC remain in the thermodynamic limit. We again expect special features (jumps, divergences) in the spectra at the respective boundaries, occurring at A, B, C for $q = \pi/2$ (Fig. 7). Fig. 8 shows neutron spectra on CPC for two field values. They indeed seem to exhibit structure in the vicinity of these points. More experiments should be performed on substances with lower critical fields, in order to test a wider field range and to see the shift of the zero energy mode at q^* with h .

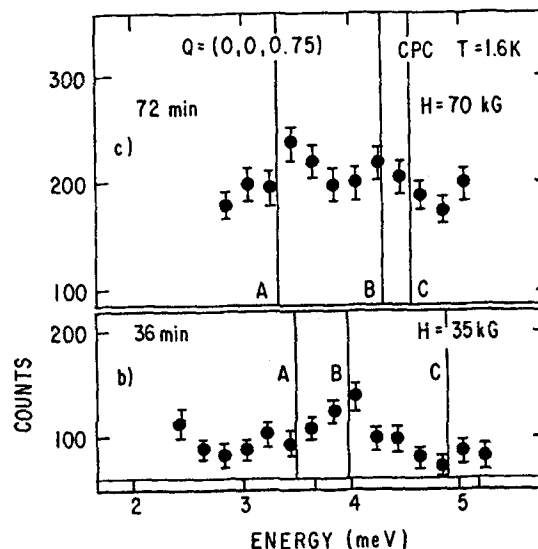


Fig. 8 Neutron cross sections on CPC in a field; a : $H = 35$ kG ($h = 0.105$), b : 70 kG ($h = 0.21$).

Finite chain data suggest the most important low frequency contribution to G_x to be at $q = \pi$. This leads to a divergent $\phi_x(0)$ at $h = h_c$ (Fig. 9) in good agreement with NMR experiments [30]. A Bulaevskii approximation to the interacting Fermion chain has produced a similar behavior [23].

Another interesting field effect shows up for $\Delta > 1$ [31]. In this range there is a "lower critical field" h_1 , such that the magnetization σ is zero for $h < h_1$ [20], and the gap in the excitation spectrum closes at h_1 . For $h > h_1$ there is again a zero energy mode at $q^* = \pi(1 - \sigma)$. This suggests searching for materials with $\Delta \geq 1$, which would show this behavior ($\Delta = 10$ for CsCoCl_3 requires too high fields).

(c) $T > 0$

Besides $G_z(q, \omega, T)$ for $\Delta = 0$, which is known exactly [16,17] there are finite chain data and Luttinger model calculations [26] available for $T > 0$. Finite chain work has been used to evaluate $\phi_x(\omega)$ and $\phi_z(\omega)$ [30] at various temperatures, see Fig. 9. The gradual build-up of the divergence at h_c is in good agreement with NMR data for T_1 on CuSeO [30], which clearly demonstrates the usefulness of these numerical methods at $T > 0$. In fact many quantities can be obtained from finite chains more reliably at $T > 0$ than at $T = 0$, since in general more states contribute, which diminishes the drawback of dealing with a discrete spectrum.

As an alternative approach the theory of "finite temperature excitations", proposed for interacting Bosons in 1d [32], has been developed for $|\Delta| > 1$ [33] and $|\Delta| < 1$ [34]. This is a generalization to finite T

of the calculation of low lying excited states, which led to the lower boundaries of excitations for $T = 0$ [10,28]. It predicts, for example, that for $0 \leq \Delta \leq 1$ there should be zero energy (finite temperature) excitations at a wave vector $q^*(T)$ like those at $q^*(h)$, discussed under (b). More specifically, for $h \gg T$, $q^*(h,T) - q^*(h,0)$ is expected to vary with T^2 to leading order in T [34]. Unfortunately the relevance of such "finite T elementary excitations" for dynamic correlation functions is not clear. On the other hand finite chain analysis [35] suggests that, in some sense, finite (small) T has a similar effect on the frequency spectrum of $G_r(q,\omega)$ as small h , which makes the existence of a q^* depending on h and T plausible. The importance of low energy contributions to G_r is also reflected in $\chi_r(q)$ which strongly weights low frequencies. Thus, for $\Delta = 0$ and 1, $\chi_z(q,T) -$ as a function of $T -$ has a maximum at some $q_m(T)$ (at $T = 0$, χ_z diverges at $q = \pi$). However, there seems to be no quantitative agreement between $q_m(T)$ and $q^*(T)$. The same holds true for $G_z(q,\omega,T)$ for $\Delta = 0$, where the low frequency tail, developing for $T > 0$ at $q \neq \pi$, would seem to reflect the low lying finite T excitations, but there is no obvious quantitative link with the theoretical prediction for $q^*(T)$ [36].

Recently, there has been growing interest in fully anisotropic chains, without any rotational symmetry in spin space (symmetry breaking is achieved by $\gamma \neq 0$ in (1) or by a field in an arbitrary direction). The theoretical analysis has almost exclusively been done by classical methods. Non-linear equations of motion in the continuum approximation show, under suitable circumstances, soliton solutions which give rise to characteristic features in $G_r(q,\omega)$ [37,38,39]. Various aspects of statics and dynamics of anisotropic quantum spin chains (e.g. $\gamma \neq 0$, $\Delta = 0$) are presented in another contribution to this conference [40]. One of the major goals is, of course, to investigate the existence and the relevance of solitons in a quantum system.

Concluding, we hope to have demonstrated the existence of striking quantum effects in 1-d spin dynamics. Some of these have already been unravelled by experiments, but other theoretical predictions have yet to be verified. This certainly calls for the search of new quasi 1-d materials with such interaction parameters as

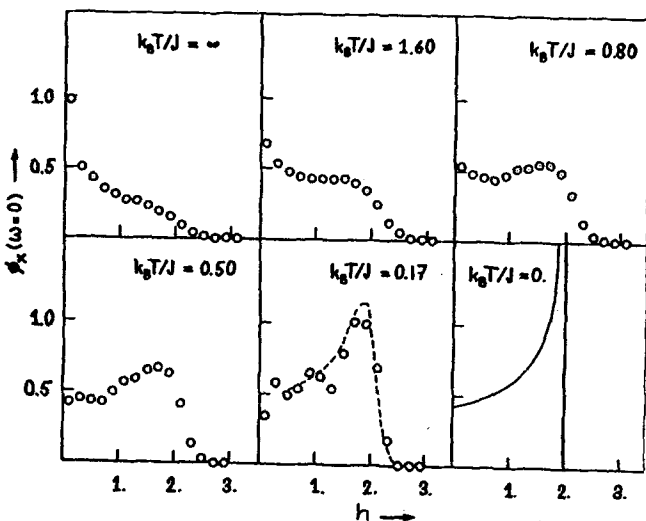


Fig. 9 Field dependence of $\chi_x(0)$ at various T from finite chain calculations ($h = 2$ is the critical field). The $T = 0$ curve results from our SWC approach.

to make the observation of various quantum effects feasible. This specially concerns the choice of anisotropy (Δ, γ) and the desire to have systems with comparable interactions but different spin quantum numbers.

It is a pleasure to thank J.C. Bonner, M. Fowler and H. Thomas, in collaboration with whom much of the work reported here has been done.

REFERENCES

- a) Supported by the Swiss National Science Foundation.
1. M. Steiner, J. Villain, C.G. Windsor, *Adv. Phys.* **25**, 87 (1976).
2. G. Reiter, A. Sjölander, *Phys. Rev. Lett.* **39**, 1047 (1977).
3. M. Blume, G.H. Vineyard, R.E. Watson, *Phys. Lett.* **50 A**, 397 (1975).
4. H.J. Mikeska, *Phys. Rev. B* **12** 2794 (1975).
5. E.H. Lieb, T. Schultz, D.C. Mattis, *Ann. Phys.* (N.Y.) **16**, 407 (1961).
6. A. Luther, I. Peschel, *Phys. Rev. B* **12**, 3908 (1975).
7. H.C. Fogedby, *J. Phys. C* **11**, 4767 (1978).
8. H.A. Bethe, *Z. Physik* **71**, 205 (1931).
9. L. Hulthen, *Arkiv Mat. Astron. Fysik* **26 A**, 1 (1938).
10. J. des Cloizeaux, J.J. Pearson, *Phys. Rev.* **128**, 2131 (1962).
11. J. des Cloizeaux, M. Gaudin, *J. Math. Phys.* **7**, 1384 (1966).
12. G. Müller, H. Beck and J.C. Bonner, *Phys. Rev. Lett.* **43**, 75 (1979).
13. G. Müller, H. Beck and J.C. Bonner, *J. Appl. Phys.* **50**, 7404 (1979).
14. J.D. Johnson, S. Krinsky, B.M. McCoy, *Phys. Rev. A* **8**, 2526 (1973).
15. P.C. Hohenberg, W.F. Brinkman, *Phys. Rev. B* **10**, 128 (1974).
16. Th. Niemeijer, *Physica* **36**, 377 (1967).
17. S. Katsura, T. Horiguchi, M. Suzuki, *Physica* **46**, 67 (1970).
18. G. Müller, H. Thomas, M.W. Puga and H. Beck, to be published.
19. H.G. Vaidya and C.A. Tracy, *Physica* **92 A**, 1 (1978).
20. C.N. Yang and C.P. Yang, *Phys. Rev.* **151**, 258 (1966).
21. M.T. Hutchings, G. Shirane, R.J. Birgeneau, S.L. Holt, *Phys. Rev. B* **5**, 1999 (1972).
22. P.M. Richards, F. Borsa, *Sol. State Comm.* **15**, 135 (1974).
23. J.P. Groen, H.W. Capel, J.H.H. Perk, T.O. Klassen, N.J. Poulis, *Physica* **97 B**, 126 (1979).
24. N. Ishimura, H. Shiba, *Progr. Theor. Phys.* **63**, 743 (1980).
25. S.K. Satija, G. Shirane, Y. Yoshizawa, K. Hirakawa, *Phys. Rev. Lett.* **44**, 1548 (1980).
26. A. Luther, I. Peschel, *Phys. Rev. B* **9**, 2911 (1974).
27. N. Ishimura, H. Shiba, *Progr. Theor. Phys.* **57**, 1862 (1977).
28. M.W. Puga, *Phys. Rev. Lett.* **42**, 405 (1979).
29. G. Müller, H. Thomas, H. Beck, J.C. Bonner, to be published.
30. J.P. Groen, T.O. Klaassen, N.J. Poulis, G. Müller, H. Thomas, H. Beck, *Phys. Rev. B*, to appear.
31. M. Fowler, M.W. Puga, *Phys. Rev. B* **18**, 421 (1978).
32. C.N. Yang, C.P. Yang, *J. Math. Phys.* **10**, 1115 (1969).
33. J.D. Johnson, *Phys. Rev. A* **9**, 1743 (1974).
34. M.W. Puga, *J. Math. Phys.* **21**, 2307 (1980).
35. G. Müller, unpublished.
36. M.W. Puga, unpublished.
37. H.J. Mikeska, *J. Phys. C* **11**, L29 (1978).
38. K.M. Leung, D.L. Huber, *Sol. State Comm.* **32**, 127 (1979).
39. H.J. Mikeska, *J. Phys. C* **13**, 2913 (1980).
40. J. Kurmann, G. Müller, H. Thomas, M.W. Puga, H. Beck, *J. Appl. Phys.*, to appear.